



Formulated poly (butyl vinyl ether) adhesives as alternative materials for direct ink writing (DIW) 3D printing

Anh Nguyen, Department of Chemical and Biomolecular Engineering, Department of Materials Science and Engineering and Institute for Advanced Materials and Manufacturing (IAMM), The University of Tennessee, Knoxville, TN 37996, USA

G. M. Fazley Elahee, and Xiang Cheng, Department of Macromolecular Sciences and Engineering, Case Western Reserve University, Cleveland, OH 44106, USA

Charles Patten, Department of Chemical and Biomolecular Engineering, Department of Materials Science and Engineering and Institute for Advanced Materials and Manufacturing (IAMM), The University of Tennessee, Knoxville, TN 37996, USA

Lihan Rong, and Chase Breting, Department of Macromolecular Sciences and Engineering, Case Western Reserve University, Cleveland, OH 44106, USA
Jose Bonilla-Cruz, and Tania Ernestina Lara Ceniceros, Advanced Functional Materials and Nanotechnology Group, Centro de Investigación en Materiales Avanzados S. C. (CIMAV-Unidad Monterrey), 66628 C.P. Apodaca, Nuevo León, Mexico

Zane Smith, Department of Chemical and Biomolecular Engineering, Department of Materials Science and Engineering and Institute for Advanced Materials and Manufacturing (IAMM), The University of Tennessee, Knoxville, TN 37996, USA

Jin Ge, Mingwei Xu, and Matthew Yang, Department of Macromolecular Sciences and Engineering, Case Western Reserve University, Cleveland, OH 44106, USA

Rigoberto Advincula¹, Department of Chemical and Biomolecular Engineering, Department of Materials Science and Engineering and Institute for Advanced Materials and Manufacturing (IAMM), The University of Tennessee, Knoxville, TN 37996, USA; Department of Macromolecular Sciences and Engineering, Case Western Reserve University, Cleveland, OH 44106, USA; Center for Nanophase Materials and Sciences, Oak Ridge National Laboratory, Oak Ridge, TN 37830, USA

Address all correspondence to Rigoberto Advincula at radvincu@utk.edu

(Received 13 June 2023; accepted 31 August 2023; published online: 20 September 2023)

Abstract

Direct Ink Writing (DIW) is a promising 3D printing method for controlled multi-material deposition to make well-defined geometrical structures. Stringent rheological requirements enable the additive build-up of extruded layers. Although commercially available, no occasion has been reported on poly(butyl vinyl ether) adhesives for DIW. The moisture curing mechanism and thixotropic build-up indicate an alternative route to cross-linking curing to thermoset elastomers. Chemical composition and rheological characterizations were conducted to evaluate printability and physicochemical properties (i.e., dielectric properties, thermal conductivity, etc.) to address the potential for further reformulation and study with nanomaterial additives.

Introduction

Additive Manufacturing (AM) methodologies enable structural deposition and layering of materials in three-dimensional (3D) complex geometries ranging from macro to microscale features. The advantage of AM in next-generation manufacturing is that it brings multidisciplinary science fields on a path of materials property development and geometric design complexity convergence.^[1] Many material extrusion-based AM methods have parallel developments in ink or paste materials with specific viscosity and curing requirements. One of these methods, called Direct Ink Writing (DIW) or viscous solution printing (VSP), has the potential for a wide range of materials that can be applied for complex deposition and structures. DIW extrudes the materials through a narrow tip or nozzle to build a layer-by-layer structure in a computer numerical control (CNC) or robotic multi-axis machine and movement. Patterning is controlled precisely through computer-aided and spatiotemporal features allowing printing materials with complex designs. Inks

must have paste-like and thixotropic viscosity, which can limit various ink chemistries. Thus, DIW can have challenges for industrial scalability for the lack of cost-effective commercial 3D printable inks.

First, an ideal DIW ink is expected to have shear thinning behavior when extruded through the deposition nozzle with adjustable flow control. Once deposited layer-by-layer, the materials should yield a stabilized 3D structure (sufficient yield stress and storage modulus properties). In this case, adhesive-sealant-based elastomers have the potential to be widely used in 3D printing since they can provide good interlayer bonding and higher thermal and chemical stability^[2] and are already commercially available and cost-effective. Combining the potential for printability and low cost, these adhesive-sealant elastomers can shorten the development time for new chemically tailored DIW inks that can be applied in many fields. These sealants have well-known shelf-life stability, thermal and electrical conductivity, electrical insulation, water resistance, and chemical resistance.^[3] Processing via crosslinking-induced solidification of polymers (e.g., polyurethane, epoxy, silicone, and acrylic) helps 3D printability at room temperature. Other polymer-based adhesives and sealants of viscous and elastomeric polymers

Rigoberto Advincula was an editor of this journal during the review and decision stage. For the MRS Communications policy on review and publication of manuscripts authored by editors, please refer to <http://www.mrs.org/editormanuscripts/>.

solidify with solvent evaporation or physical cross-linking or derivatized with moisture-curing silanes. Poly(butyl vinyl ether) is such a polymer. It is based on dispersions of various homopolymer and copolymer ratios with alkyl and hydrophilic groups, linear and branched derivatives, molecular weight (MW), and polydispersity to account for its adhesion and “tacky” properties. These formulated adhesive-sealant-based elastomers offer attractive mechanical properties while providing excellent interlayer bonding and high thermal and chemical stability.^[3] Their commercial availability makes them potential candidates for applications as cost-effective DIW 3D Printing feedstock sources.^[4] Compared to acrylic-based single-component thermosets and elastomers, these polyvinyl ether (PVE) materials can significantly reduce energy consumption during processing owing to their intrinsic solidification mechanisms, which enable curing processes at room temperature.^[4]

Nonetheless, evaluation as ink for DIW printing requires an extensive compilation of viscosity, chemical, and mechanical properties that can lead to optimized manufacturing for these classes of polymer formulations. Herein, we present a comprehensive study on the PVE-based sealant elastomers evaluating their viscoelasticity and extrusion behavior for DIW printing, investigating the role of curing, aging, and optimizing printing parameters. Additionally, we report qualitative and quantitative analysis of all the elastomers’ chemical composition and the mechanical, thermal, electrical, and adhesion performance of 3D printed objects. An essential goal of this study is to define the composition-viscosity nexus that enables the PVEs to be more widely used for 3D printing and define the potential for property optimization and applications.

Materials and methods

Materials

NovaBond commercial hybrid composite sealant was procured directly from the manufacturer, Novagard Solutions, 5109 Hamilton Ave, Cleveland, OH, and Gorilla Construction Adhesive was purchased from the local hardware store. Both were used as is without reformulating or the addition of solvents.

The reported attributes of the materials are as follows: Elastomer A (Gorilla) is a tough, versatile, all-weather, long-lasting, heavy-duty adhesive. This adhesive contains mostly Poly (butyl vinyl ether), carbonic acid, stearic acid, and phthalate-based plasticizer filled with inorganic particles, Limestone, quartz, and calcium salt.^[5] Elastomer B (NovaBond) is a ready-to-use hybrid adhesive sealant that acts as a powerful bond to substrates dissociating the need for a primer. It is a non-corrosive, single-component, MS (modified silicone) polymer hybrid sealant/adhesive.^[6] This elastomer comprises mostly Poly (butyl vinyl ether) and other components such as amorphous silica, vinyl trimethoxy silane, Bis (2-ethylhexyl) benzene-1, 4-dicarboxylate, and titanium dioxide. It is waterproof, all-weathered, and paintable that can endure extreme flexibility. In addition, it yields excellent resistance to shrinking and cracking.

Methodology

Fourier Transform Infrared Spectroscopy (FTIR) and Pyrolysis-gas chromatography-mass spectroscopy (Py-GC-MS) were used to analyze each sample’s functional group and compositions. In addition, Thermogravimetric Analysis (TGA) was done to analyze the thermal decomposition of each material component and its overall thermal degradation behavior over a temperature range. Scanning Electron Microscopy (SEM) and X-ray dispersion (EDX) Spectroscopy were used to describe each sealant and adhesive’s morphology and elemental composition. In addition, the viscosity behaviors were investigated via a parallel plate rheometer. For the post-printing characterization, the 3D printed parts were utilized to evaluate their mechanical properties using testing characterizations such as curing, durometer hardness, compression deflection, Young’s modulus, tensile strength, dielectric properties, and thermal conductivity. A more detailed description of the methodology and instrumentation combined with all the printing dimensions can be found in Supplementary Information (SI).

Results and discussion

GC-MS pyrolysis and FT-IR

As shown in Fig. S1(a), The GC-MS for Elastomer A shows two significant peaks starting from 150 to 300°C and 350 to 500°C based on evolved gas analysis (EGA). These peaks represent the dodecyl phthalate plasticizers and Poly (butyl vinyl ether). Similarly, in Fig. S1(d), the primary degradation peaks for Elastomer B are observed from 150 to 300°C and 350 to 500°C. These peaks also represent Dodecyl phthalate plasticizers and Poly(butyl vinyl ether).^[7] Several significant peaks were observed in the pyrograms by flash pyrolysis chromatography in Fig. S1(b) and Fig. S1(e) for Elastomer A and B, such as the dodecyl phthalate plasticizer and its decomposed moieties. Peaks attributable to UV-328, (2-(2H-benzotriazol-2-yl)-4,6-di-tert-pentylphenol), a common phenolic benzotriazole UV stabilizer additive, can also be found in both composites. The peaks of about 4.5 min. to 7.5 min. retention times are attributed to the pyrolysis of poly (butyl vinyl ether).^[8] Traces of silane or silica composition could be found between 500–700 °C range of the EGA though not easily resolvable with library matching. Assignments were done using the F-Search Library match (Frontier Laboratories). The FTIR spectrum, Fig. S1(c), supports the presence of poly (butyl vinyl ether), which shows the functional peaks of C-H and C-O at 2800–3000 cm^{-1} and 1200–1400 cm^{-1} , respectively.^[9] For Elastomer B, Fig. S1(f), the functional group of Si-O-Si is observed at around 800 cm^{-1} , which confirms the presence of trimethoxy vinyl silane, 3-aminopropyltriethoxysilane, 3-(trimethoxysilyl)propylamine.^[10] For Elastomer A, the spectra observed at 1100 cm^{-1} are expected to be O-Si-O, which can come from silica particles present.^[11] This latter component could be for rheology modification and maintenance of thixotropy on the original formulation. Both however confirm a large peak at 1475 cm^{-1} region attributable to calcite or calcium carbonate minerals.

Polymer curing mechanism

As a result of the GC–MS pyrolysis, both Elastomer A and Elastomer B contain poly(butyl vinyl ether), which is in the polyvinyl ethers (PVE) class. The main applications of vinyl ether copolymers are adhesives, release and surface coatings, lubricants, elastomers, etc. Polyvinyl ethers, once modified with silicones, called modified silicone (MS) polymer, are viscous oils or tacky adhesives. Both elastomers are MS polymers. Their curing mechanism is through a process called moisture-triggered curing. MS polymers are very flexible, which enables them to expand and contract with changes in temperature and humidity and adsorb the vibrations from structural movement, impact, and sound. Combined with UV stability and abrasion resistance like polyurethanes, MS polymer sealants have high durability and weather resistance. Their high-performance capabilities make MS polymer sealants well-suited to many applications encountered by many industries.^[12]

Thermo-gravimetric analysis TGA

Figure 1(a) shows that Elastomer A has three degradation peaks. Over the interval from 25 to 350°C, there appears to be an 8 wt% loss which is attributed to the degradation of the dodecyl phthalate plasticizer, which is expected to degrade from 250 to 350°C.^[13] The second peak for 25 wt% loss from 350 to about 450°C represents the thermal degradation of the poly (butyl vinyl ether).^[14] The following weight loss of 28 wt% extends from about 500 to 700°C showing the presence of inorganic compounds that tends to degrade at such high temperatures, up to 800°C. On the other hand, For Elastomer B, Fig. 1(b), an initial peak is observed from 140 to 350°C is seen, which exhibits the evaporation of residual monomer, n-butyl vinyl ether, which has the thermal decomposition starting from 317 to 377.0°C.^[7] The next degradation peak at 20.1 wt% shares a similar trend as Elastomer A, which is the initial degradation of poly butyl vinyl ether from 350 to 450°C. The last peak from about 500 to 800°C also

shows the inorganic filler conversion of CaCO₃ to CaO, which is expected to be obtained from 600 to 800°C.^[15] Higher than 750°C represent other solid additives like TiO_x, silica particles, clay, etc., supported by the EDX measurements.

SEM/EDX

The SEM image of Elastomer B is depicted in Fig. 2(a). Based on the SEM images, it is seen that Elastomer B has a rough surface with a high percentage of filler composite. Rough patches are the depiction of organic filler within the polymeric matrix. On the other hand, EDX images are used to analyze the relative elemental compositions in the Elastomer B. Figure 2(b) shows the percentage compositions of Elastomer B. In contrast, Fig. 2(c–i) depicts the spatial distribution for each elemental mapping through EDX analysis. Based on the relative formulation design of the adhesive materials, a significant percentage of C, O, and Ca can be observed with the mass percentage respectively at 36.80%, 36.81%, and 21.50% for Fig. 2(c–e). Of course, the amount of C is attributed to the adhesive polymer matrix poly(butyl vinyl ether), which has C, H, and O elemental composition. This also indicates the presence of CaCO₃ (Limestone) as a primary additive. Figure 2(f–i) represents the other elements, Mg, Si, P, and Ti, which could be the composition of other additives or impurities due to their low mass percent in the polymeric matrix. The SEM image of Elastomer A can be observed in Fig. S2(a), along with its elemental composition analyzed by EDX. The presence of C, O, and Ca was shown through spatial distribution via elemental mapping. All three elements comprise the most composition of Elastomer A's formula with the mass percentage at 37.71%, 37.94%, and 20.88%, respectively. Since Elastomer A contains mainly limestone, carbonic acid, and calcium salt from 30 to 60 wt% and 10 to 30 wt%, respectively,^[6] the other elements found from EDX, Fig. S3(c–h), indicate the impurities found or minor additives (silica) due to a meager mass percentage compared to C, O, and Ca.

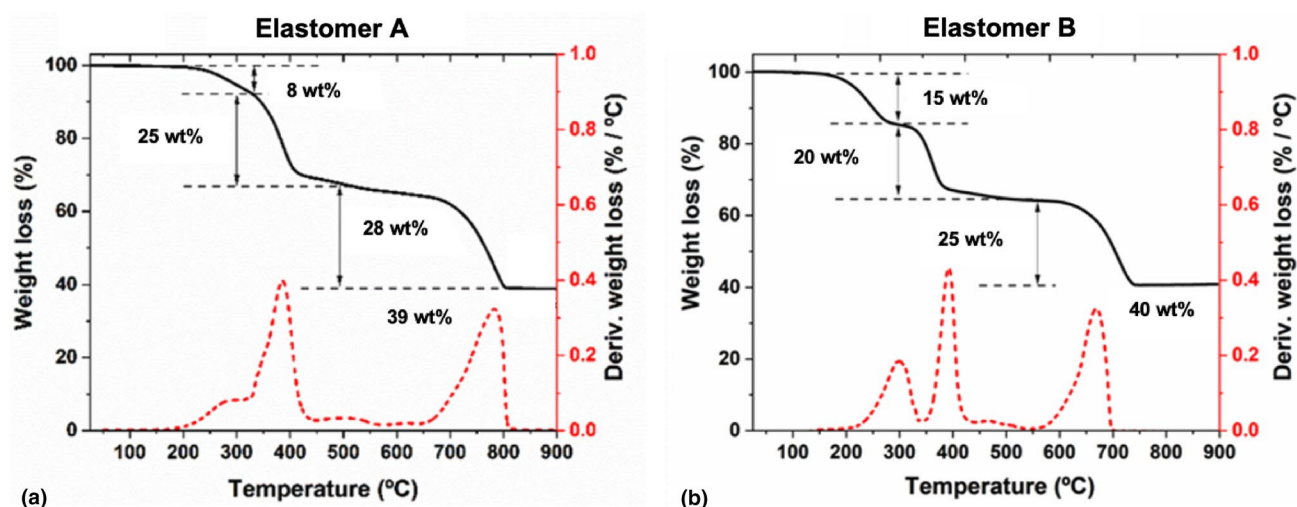


Figure 1. Thermal degradation was used to analyze the compositions of the Elastomers. TGA graphs of (a) Gorilla or Elastomer A; (b) NovaBond or Elastomer B showing the major thermal degradation transitions. Note the almost similar solid weight % of additives.

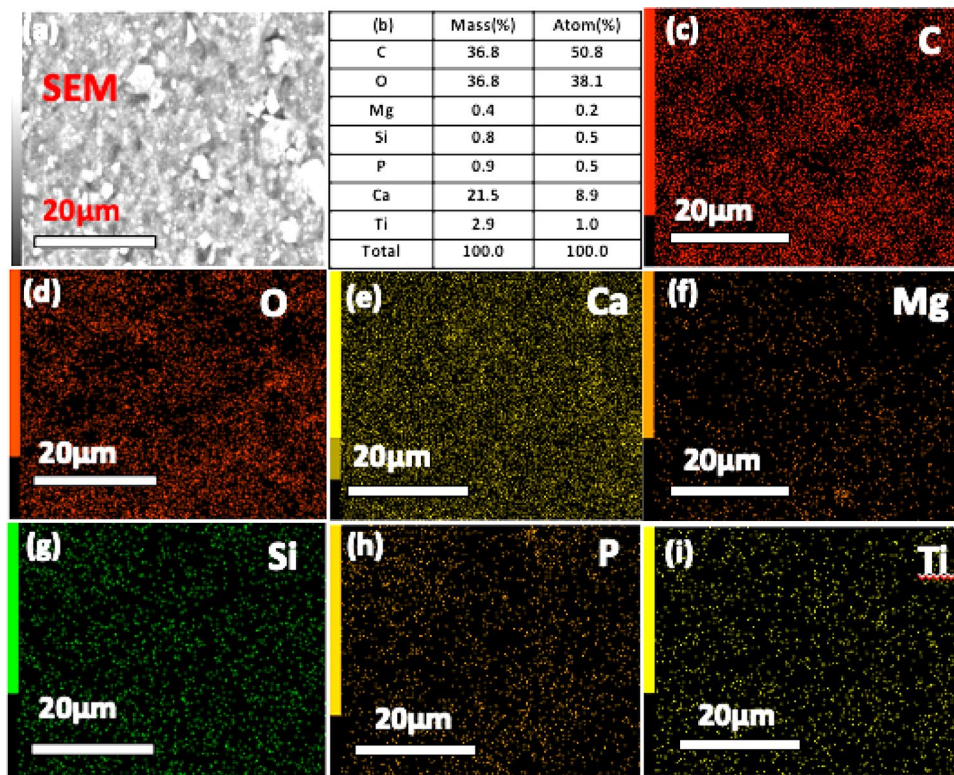


Figure 2. SEM microscopy investigated the morphology and roughness of the samples. SEM–EDX images of Elastomer B: (a) SEM micrograph, (b) Calculated elemental %, (c–i) elemental mapping. The importance of elemental mapping is in confirming the presence of fillers and additives commonly associated with formulated sealant-adhesive resins.

The EDX elemental composition’s importance confirms the mineral fillers’ presence and roles that contribute to the viscosity and thixotropic behavior, including the density necessary as a suitable sealant and adhesive material. The high weight % (40%), as described by the TGA data, confirms their presence and typical commercial formulation.

Viscosity

Elastomer A and Elastomer B have similar patterns for the viscosity versus log shear rate patterns in [Fig. 4(a, b)]. However, it can still be observed that Elastomer B has a slightly lower viscosity. From both TGA data, since Elastomer A has higher filler content, 39%, plus non-cross linkable monomer content, 25 wt% than those of Elastomer B containing 34 wt% filler content and 20.1 wt% non-cross linkable monomer. In addition. From Fig. 4(c), Elastomer A’s thixotropic index is also higher than Elastomer B, which supports how the more viscous the material, the more thixotropic it is, which is highly desirable due to their correlation pattern layering during and post-printing. This higher thixotropic index adds more value to the shear-thinning behavior of these properties. It is essential for higher commercial-speed 3D printing processes. Future rheological studies will include storage and loss modulus measurements, tan delta. It is necessary for reformulation with other additives. Such studies are expected to give a better viscoelastic description

and correlation with the molecular weight (or blended nature) of the PVEs used.

DIW printing

The commercially available poly (butyl vinyl ether) elastomers were applied as inks for DIW in different shapes shown in Fig. 3(a). Many attempts were made to adjust the printing parameters to obtain the best resolution for printing these two construction elastomers. Figure 3(a) shows the best results of printing these 2 elastomers as an alternative to expensive chemically tailored ink for DIW. Many modifications were made to obtain the best printing resolution. Increasing the extrusion rate parameters, in this case, involves increasing the nozzle pressure to add strain to the stepper motor. It will be necessary to use more predictive methods for optimization of slicing, G-code modification, printing parameters (bed height, speed, nozzle size) to shorten this development phase especially with future toolpath precision in multi-axis printing set-ups.

A simplistic dynamic fluid model Fig. 3(c) to simulate relationships between how the viscosity of the fluid (μ), the internal radius of the nozzle (R_s), print speed (v_o), the height of the printed pattern (h), tapered zone length (h_z) and driving pressure (P) can affect the width of deposited fluid (a) is shown using Eq. 1.

$$a = \frac{\pi R_s P}{8\mu v_o h h_z} \quad (1)$$

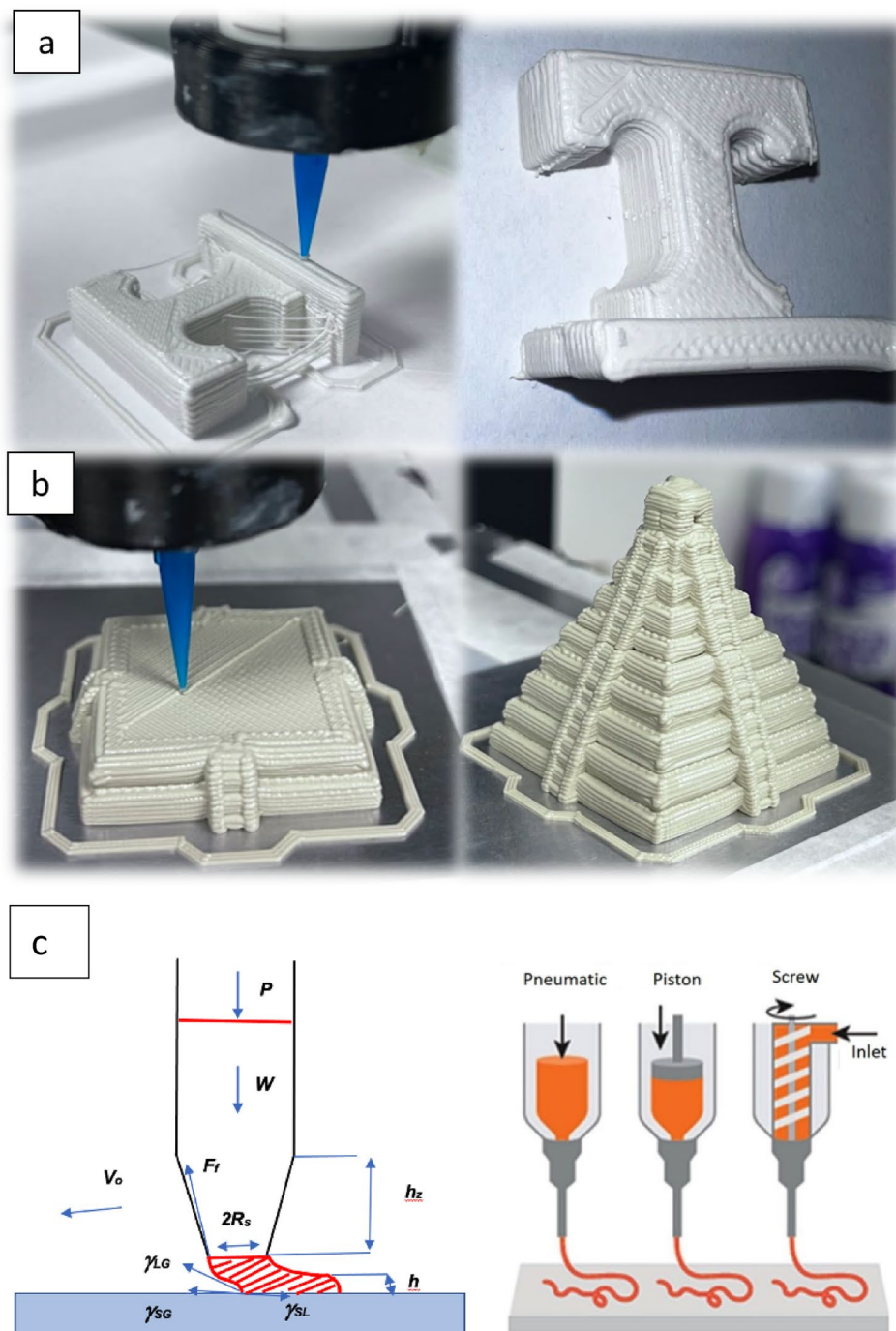


Figure 3. Optimization of the 3D printing parameters is necessary to demonstrate scalability and complex geometries. High-resolution printed samples for (a) Elastomer A; (b) Elastomer B with optimization. A simplistic dynamic fluid model can be used to identify parameters for optimization (c).

The forces governing the dispensing process include the air pressure, the nozzle wall friction, and the polymer's surface tension. Based on the fluidity of the material, Eq. 1 could estimate the dimensions of the deposited material. Further discussions are given in the Supporting Information (SI) material.

Compression-deflection

The 10% and 30% compressive-deflection test results are shown in [Fig. 4(d, e)]. For 10% and 30% deflection, Elastomer B yields the lowest compression stress at 0.18 MPa and 0.37 MPa, respectively. This explains the smaller weight percent

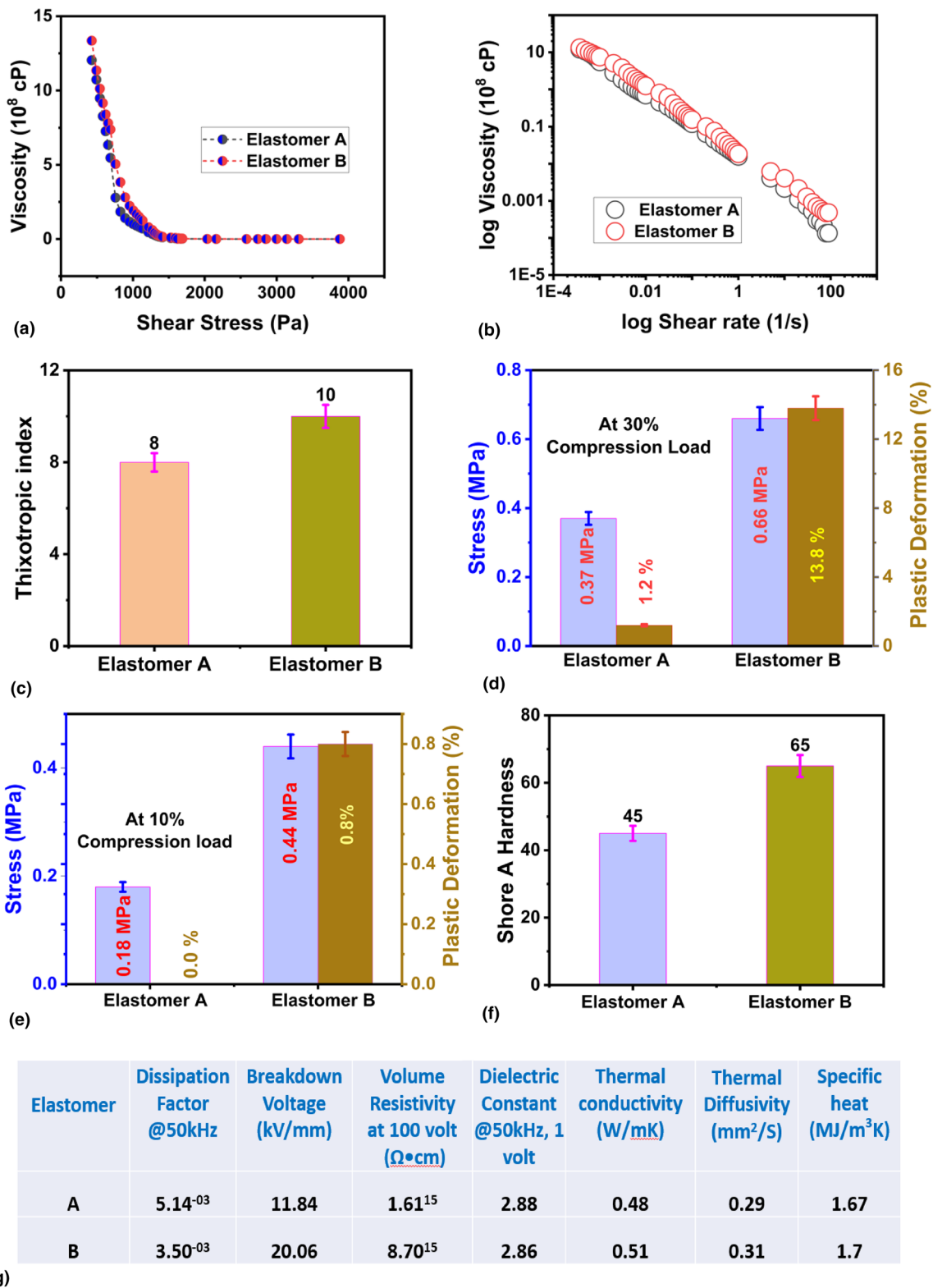


Figure 4. Characterization data for both Elastomer A and Elastomer B: (a) Viscosity over shear rate in a log scale; (b) log viscosity over shear rate in a log scale; (c) Thixotropic index; (d) 10% compression deflection; (e) 30% compression deflection; (f) shore A durometer hardness and (g) dielectric properties and breakdown voltage. The comparison of both elastomers side-by-side indicates the differences in their formulation and how it affects their properties, although both have excellent printability.

of the filler of Elastomer B compared to Elastomer A, as smaller filler content gives less impact-resisting changes to compression deflection. For plastic deformation, only under 30% deflection that Elastomer B experiences any changes at 1.2 MPa.

On the other hand, Elastomer A yields higher compression stress for 10% and 30%, respectively, at 0.44 MPa and 0.66 MPa. Higher compression shows higher filler content, which is sufficient to show that resistance changes to compression deflection. This also shows the same trend for plastic deformation, in which Elastomer A has a higher deformation % compared to Elastomer B at 0.8% and 23.8% at 10% and 30%, respectively. Such high plastic deformation could be due to the irreversible deformation of the filler layering up along with the non-crosslinked matrix.

Durometer hardness

Shore, A hardness of Elastomer A, Fig. 4(f), yields higher than that of Elastomer B. Higher hardness represents higher crosslinking within the materials, which also has the higher filler content and vice versa for Elastomer B. In addition, lower hardness indicates more elasticity due to a lower degree of crosslinking across the polymeric matrix. The balance of this uncross-linked silane content can act more as a plasticizer. Therefore, the lower hardness of Elastomer B results in higher elasticity and better flowability during printing.

Tensile testing

Tensile testing requires the maximum stress the materials can endure until it breaks down. Based on Fig. S2(e), Elastomer A can endure more stress than Elastomer B at 528.6 Psi compared to 171.75 Psi. Tensile testing can indicate the level of crosslinking density. The higher the tensile stress, the more crosslinking density, making it harder to tear the tensile bar. Therefore, the hardness of Elastomer B is lower. This is relevant to the amount of filler in Elastomer A, as confirmed by TGA, at 40 wt% compared to Elastomer B at 34 wt%. The tensile properties are also consistent with the durometer hardness.

Young's modulus

Fig. S2(a) shows the calculated Young's Modulus values for all the samples. Elastomer A yields a higher Young's Modulus at 0.03 MPa than Elastomer B at 0.01 MPa. These Young's Modulus values indicate each elastomer's stiffness for the materials post-printing. Therefore, Elastomer A gives higher cross-linking density and interfacial bonding between the filler and polymeric matrix.^[16]

Dielectric constant

Dielectric Constant is used to determine the ability of an insulator to store electrical energy. The dielectric constant is the ratio of the capacitance induced by two metallic plates with an insulator between them to the capacitance of the same plates with air or a vacuum between them. The dielectric constant at

50 kHz, 1 V in Figure 4(g) shows the electric potential energy, which is the ratio of the capacitor within the materials as the dielectric vacuum (or air) as the dielectric.^[17] A lower dielectric constant shows that the polymeric matrix within the elastomers can be protected from heating while being exposed to a high electric field. In this case, Elastomer A has a higher dielectric constant, indicating higher heat absorption under any high electric field. If a material were strictly insulated, it would be better to have a lower dielectric constant.

Dissipation factor

The dissipation factor (DF) is the property related to the effectiveness of insulating materials. In other words, it is described as the ratio between the permittivity and the conductivity of the materials.^[18] Dissipation happens when the energy within the electric field is lost due to the "internal motions" of the materials.^[19] It is essential to measure the dissipation factor as it can be crucial in applications such as cables' insulation, encapsulation for electric components, interlayer dielectric, and printed wiring board materials. These inks should yield a deficient dissipation factor to fit in those applications. Figure 4(g) shows as low as 0.01 for both elastomers, which is ideal in this case. Since DF is the reciprocal of the ratio between the insulating materials' capacitive reactance to its resistance at a specified frequency, it measures the inefficiency of an insulating material.

Breakdown voltage

Breakdown voltage is the threshold voltage that causes the breakdown preventing current flow.^[20] Breakdown strength is essential in determining the energy storage density of nanocomposites. In this case, the breakdown voltage can indicate how the matrix is crosslinking with the non-conductive fillers. Figure 4(g) shows that the breakdown voltage for Elastomer B, 16.2 kV/mm, is higher than Elastomer A, 9.72 kV/mm. This confirms that Elastomer A has more plasticizer content with less non-conductive fillers.

Thermal conductivity

Thermal conductivity measures the rate of transfer energy across a unit surface area.^[21] Therefore, in this case, it calculates how much heat can flow through the printed elastomers. From Figure S2, Elastomer A and Elastomer B have similar thermal conductivity, at 0.51 and 0.48, respectively. Elastomer A has a higher thermal conductivity due to higher crosslinking density. Since covalent bonds form the cross-links in polymer crosslinking, the phonon transport is enhanced, which increases thermal conductivity.^[22]

Peel adhesion strength

Based on the average peel adhesion strength, Elastomer B exceeds more than Elastomer A for all the tests done on 3 substrates, Stainless steel, PVC, and ABS. ABS gives the lowest peel strength for both elastomers among all the substrates—lower peel adhesion strength results from various mechanisms

within each elastomer. In addition, the adhesive matrix plays an essential role in each elastomer's peel strength. Since Elastomer B has the highest average peel strength overall compared to Elastomer A, this could confirm how Elastomer B overall has more polymer matrix bonding due to their higher percentage of crosslinked polymers based on the TGA result in Fig. 1(b)

Sample curing and dimensional stability

For the sample curing and shrinkage measurements, the following procedure was done. Uniform printed parts (disk shape) were utilized to investigate their shrinkage over time at room temperature. The dimensional stability was measured against the original CAD dimensions with a caliper. The time range is from the freshly printed sample up to 10 days. It was observed that Elastomer A has a lower shrinkage percentage at 0.5 wt% compared to Elastomer B at 5.0 wt%. The shrinkage is attributed to the evaporation of water during curing. The high shrinkage indicates that Elastomer B contains a lower polymer matrix and solid wt% composition with more solvent than Elastomer A. Elastomer A is most likely 100% solvent free see Figure S2.

Conclusions

Several studies have been conducted on various DIW materials, including hydrogels, thermoset elastomers, vitrimers, acrylates, etc.^[23–32] This study showed the viability of poly alkyl vinyl ether-based adhesives and sealants as additional materials that can be utilized for DIW. As currently formulated, these elastomers can be printed with the optimization of the DIW printers using modular printing heads. Two types of commercial elastomer adhesive sealants were investigated. Both gave high-resolution printability with excellent thermo-mechanical properties and thermal stability. Comparisons with the two elastomers showed the effect of higher solid weight % compositions on crosslink ability and thermo-mechanical properties, i.e., higher weight% resulted in higher tensile properties, Young's modulus, lower shrinkage, etc. Aging and curing tests show they can maintain their material's performance under higher temperatures. The shrinkage volume is related to solid weight %, which is a higher %, resulting in less shrinkage. Electrical conductivity, thermal conductivity, and dielectric properties indicate a typical sealant behavior with insulation properties with poor conductivity. Analyzing their dielectric properties can be relevant to fields and applications such as dielectric layers, batteries, electrical wires, etc.

Further studies using nanofillers (graphene, carbon nanotubes, etc.) can be done to improve their thermal, electrical, and mechanical properties post-printing, especially with the help of percolation theory in composition. It will be necessary for statistical methods and perhaps machine learning (ML) to accelerate the development of new DIW materials and testing protocols.^[33] A primary component analysis (PCA) study can also accelerate reformulation and repurposing in DIW. However, detailed rheological studies will still be needed to maintain the printability of these modified inks.

Acknowledgments

We acknowledge technical support from Frontier Laboratories and Quantum Analytics. This work (or part of this work) was conducted in Oak Ridge National Laboratory Center for Nanophase Materials Sciences (CNMS) by R C Advincula. CNMS is a US Department of Energy Office of Science User Facility.

Funding

Basic Energy Sciences.

Data availability

All data for the work is either included in this manuscript or is part of the Electronic Supplementary Information (SI) file that will be publicly available.

Declarations

Conflict of interest

There are no conflicts to declare.

Supplementary Information

The online version contains supplementary material available at <https://doi.org/10.1557/s43579-023-00477-5>.

References

1. M.A.S.R. Saadi, A. Maguire, N.T. Pottackal, M.S.H. Thakur, M.M. Maruf, A.J. Hart, P.M. Ajayan, M.M. Rahman, Direct ink writing: a 3D printing technology for diverse materials. *Adv. Mater.* **34**, 2108855 (2022). <https://doi.org/10.1002/adma.202108855>
2. D.S. Shah, B.K. Lawson, M. Yaszemski, Description and Definition of Adhesives, and Related Terminology, in *Biomaterials Science*. (Academic Press, Cambridge, 2020)
3. "Elastomeric Systems," Master Bond Elastomeric Adhesives and Sealants | MasterBond.com. <https://www.masterbond.com/products/elastomeric-systems>. Accessed 07 Mar 2023
4. S. Rouif, Radiation cross-linked polymers: Recent developments and new applications. *Nucl Instrum Methods Phys Res Sect B: Beam Interact Mater Atoms* **236**(1–4), 68–72 (2005). <https://doi.org/10.1016/j.nimb.2005.03.252>
5. NovaBond textured hybrid construction sealant specification data. https://novagard.com/wp-content/uploads/dlm_uploads/2022/08/TDS-NBT-NovaBond-TEXTURED-Hybrid-Construction-Sealant-v1.8.pdf. Accessed 07 Mar 2023
6. "Safety data sheet - gorilla construction adhesive." <https://www.gorillatough.com/wp-content/uploads/Gorilla-Construction-Adhesive.pdf>. Accessed 07 Mar 2023
7. POLYVINYL ETHERS (PVE), *Properties of polyvinylethers*. <https://polymerdatabase.com/polymer%20classes/Polyvinylether%20type.html>. Accessed 07 Mar 2023
8. H. Nakata, S. Murata, J. Filatreau, Occurrence and concentrations of benzo-triazole UV stabilizers in marine organisms and sediments from the Ariake Sea, Japan. *Environ. Sci. Technol.* **43**(18), 6920–6926 (2009). <https://doi.org/10.1021/es900939j>
9. Libretexts, "Infrared spectroscopy absorption table," *Chemistry LibreTexts*, Accessed 03 Nov 2020
10. E. Herth, R. Zeggari, J.-Y. Rauch, F. Remy-Martin, W. Boireau, Investigation of amorphous SiO_x layer on gold surface for Surface Plasmon Resonance

- measurements. *Microelectron. Eng.* (2016). <https://doi.org/10.1016/j.mee.2016.04.014>
11. Everkem Products. Introduction to MS Polymer Hybrid Sealants and Adhesives. Available: <https://everkemproducts.com/introduction-to-ms-polymer-hybrid-sealants-and-adhesives/>. Accessed 17 May 2023
 12. Y. Sainohira, K. Fujino, A. Shimojima et al., Preparation of CO₂-adsorbable amine-functionalized polysilsesquioxanes containing cross-linked structures without using surfactants and strong acid or base catalysts. *J. Sol-Gel Sci. Technol.* **91**, 505–513 (2019). <https://doi.org/10.1007/s10971-019-05072-6>
 13. K. Saido, H. Taguchi, S. Yada et al., Thermal decomposition products of phthalates with poly(vinyl chloride) and their mutagenicity. *Macromol. Res.* **11**, 178–182 (2003). <https://doi.org/10.1007/BF03218349>
 14. T.O. Bamkole, E.U. Emovon, The thermal decomposition of n-butyl vinyl ether. Part I. The inhibited reaction. *J. Chem. Soc. B* (1967). <https://doi.org/10.1039/J29670000523>
 15. K.S.P. Karunadasa, C.H. Manoratne, H.M.T.G.A. Pitawala, R.M.G. Rajapakse, Thermal decomposition of calcium carbonate (calcite polymorph) as examined by in-situ high-temperature X-ray powder diffraction. *J. Phys. Chem. Solids* **134**, 21–28 (2019). <https://doi.org/10.1016/j.jpcs.2019.05.023>
 16. D. Kuckling, A. Doering, F. Krahl, K.-F. Arndt, Stimuli-Responsive Polymer Systems, in *Polymer Science A Comprehensive Reference*. (Elsevier, Amsterdam, 2012)
 17. Z. Xu, S. Zheng, X. Wu, Z. Liu, R. Bao, W. Yang, M. Yang, High actuated performance MWCNT/Ecoflex dielectric elastomer actuators based on layer-by-layer structure. *Compos. Part A: Appl. Sci. Manuf.* (2019). <https://doi.org/10.1016/j.compositesa.2019.105527>
 18. “Dissipation factor,” *Dissipation Factor (DF) of Plastics - Unit, Formula and Measurement*. <https://omnexus.specialchem.com/polymer-properties/properties/dissipation-factor>. Accessed 07 Mar 2023
 19. X. Yu, B. Yi, F. Liu, X. Wang, Prediction of the dielectric dissipation factor $\tan\delta$ of polymers with an ANN model based on the DFT calculation. *React. Funct. Polym.* **68**(11), 1557–1562 (2008). <https://doi.org/10.1016/j.reactfunctpolym.2008.08.009>
 20. L.W. McKeen, Chapter 2 - Introduction to the Properties of Plastic and Elastomer Films, in *Plastics Design Library, Film Properties of Plastics and Elastomers*. ed. by L.W. McKeen (William Andrew Publishing, Norwich, 2012)
 21. N.G. Parsonage, Chapter 6 - Thermal Conductivity, in *The Commonwealth and International Library: Chemistry Division, The Gaseous State*. ed. by N.G. Parsonage (Elsevier, Amsterdam, 1966)
 22. M.P. Jahan, M. Rahman, Y.S. Wong, Micro-Electrical Discharge Machining (Micro-EDM): Processes, Varieties, and Applications, in *Comprehensive Materials Processing*. (Elsevier, Amsterdam, 2014)
 23. F. Elahee, L. Rong, C. Breting, J. Bonilla-Cruz, T. Cenicerros, Z. Smith, J. Ge, X. Cheng, M. Xu, M. Yang, E. Ribeiro, E. Caldona, R. Advincula, Acrylic sealants as practicable direct ink writing (DIW) 3D-printable materials. *MRS Commun.* **13**, 299–305 (2023). <https://doi.org/10.1557/s43579-023-00343-4>
 24. A. Espera, J. Dizon, A. Valino, Q. Chen, I. Silva, S. Nguyen, L. Rong, R. Advincula, On the 3D printability of silicone-based adhesives via viscous paste extrusion. *MRS Commun.* (2023). <https://doi.org/10.1557/s43579-022-00318-x>
 25. D. Gutierrez, E. Caldona, Z. Yang, X. Suo, X. Cheng, S. Dai, R. Espiritu, R. Advincula, 3D-printed PDMS-based membranes for CO₂ separation applications. *MRS Commun.* (2022). <https://doi.org/10.1557/s43579-022-00287-1>
 26. A. Stephen, S. Bhojate, P. Cao, R. Advincula, N. Dahotre, Y. Jiang, W. Choi, 3D-printed flexible anode for high-performance zinc ion battery. *MRS Commun.* **12**, 894–901 (2022). <https://doi.org/10.1557/s43579-022-00267-5>
 27. R. Advincula, J. Dizon, E. Caldona, R. Viers, F. Siacor, R. Maalihan, A. Espera, On the progress of 3D-printed hydrogels for tissue engineering. *MRS Commun.* **8**(3), 1–15 (2021). <https://doi.org/10.1557/s43579-021-00069-1>
 28. W. Niu, Z. Zhang, Q. Chen, P.-F. Cao, R. Advincula, Highly recyclable, mechanically isotropic and healable 3D-printed elastomers via Polyurea vitrimers. *ACS Mater. Lett.* **3**(8), 1095–1103 (2021). <https://doi.org/10.1021/acsmaterialslett.1c00132>
 29. F. Siacor, Q. Chen, J. Zhao, L. Han, A. Valino, E. Taboada, E. Caldona, R. Advincula, On the additive manufacturing (3D Printing) of viscoelastic materials and flow behavior: from composites to food manufacturing. *Addit. Manuf.* **5**(23), 102043 (2021). <https://doi.org/10.1016/j.addma.2021.102043>
 30. Q. Chen, J. Zhao, J. Ren, L. Rong, P.-F. Cao, R. Advincula, 3D printed multifunctional, hyperelastic silicone rubber foam. *Adv. Func. Mater.* **29**(23), 1900469 (2019). <https://doi.org/10.1002/adfm.201900469>
 31. A. Jurago, R. Viers, A. Nguyen, E. Ribeiro, A. Espera Jr., E. Caldona, R. Advincula, On the 3D printing of polyelectrolyte complexes: a novel approach to overcome rheology constraints. *MRS Commun.* (2023). <https://doi.org/10.1557/s43579-023-00415-5>
 32. C. Nocheseda, G. Elahee, M. Santos, X. Cheng, R. Espera, R. Advincula, On the 3D printability of one-part moisture-curable polyurethanes via direct ink writing (DIW). *MRS Commun.* **13**, 647–656 (2023). <https://doi.org/10.1557/s43579-023-00407-5>
 33. M. Islam, Rupom, P. Adhikari, Z. Demchuk, I. Popov, A. Sokolov, F. Wu, R. Advincula, N. Dahotre, Y. Jiang, W. Choi, Boosting piezoelectricity by 3D printing PVDF-MoS₂ composite as a conformal and high-sensitivity piezoelectric sensor. *Adv. Funct. Mat.* **5**, 2–6 (2023). <https://doi.org/10.1002/adfm.202302946>
 34. M. Espino, B. Tuazon, A. Espera Jr., C. Nocheseda, R. Manalang, J. Dizon, R. Advincula, Statistical methods for design and testing of 3D-printed polymers. *MRS Commun.* **13**, 193–211 (2023). <https://doi.org/10.1557/s43579-023-00332-7>

Publisher's Note Springer Nature remains neutral with regard to jurisdictional claims in published maps and institutional affiliations.

Springer Nature or its licensor (e.g. a society or other partner) holds exclusive rights to this article under a publishing agreement with the author(s) or other rightsholder(s); author self-archiving of the accepted manuscript version of this article is solely governed by the terms of such publishing agreement and applicable law.